Polar Auxin Transport Is Essential for Medial versus Lateral Tissue Specification and Vascular-Mediated Valve Outgrowth in Arabidopsis Gynoecia[1][W]

Emma Larsson*[2], Christina J. Roberts, Andrea R. Claes, Robert G. Franks, and Eva Sundberg*

Department of Plant Biology, Swedish University of Agricultural Sciences Uppsala BioCentre and Linnean Centre for Plant Biology in Uppsala, 756 51 Uppsala, Sweden (E.L., C.J.R., A.R.C., E.S.); and Department of Plant and Microbial Biology, North Carolina State University, Raleigh, North Carolina 27695 (R.G.F.)

ORCID IDs: 0000-0001-8042-8119 (E.L.); 0000-0002-8116-0705 (C.J.R.); 0000-0003-4228-434X (E.S.).

Although it is generally accepted that auxin is important for the patterning of the female reproductive organ, the gynoecium, the flow as well as the temporal and spatial actions of auxin have been difficult to show during early gynoecial development. The primordium of the Arabidopsis (*Arabidopsis thaliana*) gynoecium is composed of two congenitally fused, laterally positioned carpel primordia bisected by two medially positioned meristematic regions that give rise to apical and internal tissues, including the ovules. This organization makes the gynoecium one of the most complex plant structures, and as such, the regulation of its development has remained largely elusive. By determining the spatiotemporal expression of auxin response reporters and localization of PINFORMED (PIN) auxin efflux carriers, we have been able to create a map of the auxin flow during the earliest stages of gynoecial primordium initiation and outgrowth. We show that transient disruption of polar auxin transport (PAT) results in ectopic auxin responses, broadened expression domains of medial tissue markers, and disturbed lateral preprocambium initiation. Based on these results, we propose a new model of auxin-mediated gynoecial patterning, suggesting that valve outgrowth depends on PIN1-mediated lateral auxin maxima as well as subsequent internal auxin drainage and provascular formation, whereas the growth of the medial domains is less dependent on correct PAT. In addition, PAT is required to prevent the lateral domains, at least in the apical portion of the gynoecial primordium, from obtaining medial fates.

The gynoecium is a highly complex assembly comprised of different tissues that work together to support female reproductive competence in angiosperms. As such, studies of the regulatory networks controlling gynoecial development are essential to not only understand plant reproduction, but also increase our knowledge about intertissue-specific cross talk and coordinated development. A gynoecium is composed of one or more carpels, which may have evolved by the invagination of an ancestral leaf-like structure carrying spores along its edges (for review, see Hawkins and Liu, 2014). The Arabidopsis (*Arabidopsis thaliana*) gynoecium is a bilateral structure composed of two congenitally fused carpels likely derived from the fusion of two leaf-like structures in which the central domains became the lateral valves and the peripheral meristematic margins carrying the ovules became the medial tissues (Hawkins and Liu, 2014). It has been suggested that the medial domains of the Arabidopsis gynoecial primordium are partially differentiated quasi-meristems with maintained meristematic characteristics allowing for prolonged proliferation (Girin et al., 2009). Accordingly, many lateral domain-specific genes are associated with leaf development, while several genes active in the medial domains are related to meristematic activity (Dinneny et al., 2005; Alonso-Cantabrana et al., 2007; González-Reig et al., 2012).

Arabidopsis gynoecium development has been described and reviewed extensively (Sessions, 1997; Bowman et al., 1999; Ferrándiz et al., 1999; Balanzá et al., 2006; Østergaard, 2009; Sundberg and Ferrandíz, 2009) and is summarized in Figure 1. Briefly, at early floral stage 5 (stages according to Smyth et al., 1990), after the initiation of outer floral organs, the remaining floral meristem becomes dome shaped. Although the meristem still appears

[1]This work was supported by the Carl Tryggers Foundation (to E.S.), the Swedish Research Council Formas (grant nos. 229–2012–973 to E.L. and 229–2010–1002 to E.S.), the Olle Engkvist Foundation (to E.S.), the Helge Ax:son Johnson Foundation (to E.L.), The Royal Physiographic Society in Lund (to E.L.), the Selma Andersson Foundation (to E.L.), the National Science Foundation (grant Integrative Organismal Systems no. 1355019 to R.G.F.), and the FP7–PEOPLE–2013–IRSE FRUIT LOOK programme (to E.S. and R.G.F.).

[2]Present address: Molecular and Developmental Genetics, Institute of Biology Leiden, Leiden University, Sylviusweg 72, 2333BE Leiden, The Netherlands.

* Address correspondence to emma.larsson@slu.se and eva.sundberg@slu.se.

The author responsible for distribution of materials integral to the findings presented in this article in accordance with the policy described in the Instructions for Authors (www.plantphysiol.org) is: Eva Sundberg (eva.sundberg@slu.se).

E.L. designed most experiments and discussed these with E.S.; E.L. performed most experiments and analyzed data; E.L. and C.J.R. designed and C.J.R. performed and analyzed PGP-related experiments. A.R.C. participated in FIL and KNAT1 expression analyses; R.G.F. created the SHP2 construct and contributed to experimental design; E.L. wrote the article and all authors discussed the results and commented on the article.

[W] The online version of this article contains Web-only data.
www.plantphysiol.org/cgi/doi/10.1104/pp.114.245951

 © 2014 American Society of Plant Biologists. All Rights Reserved.

radially symmetric, it is considered to have a medial plane (black dashed lines in Fig. 1) facing the inflorescence meristem and a lateral plane (white dashed lines in Fig. 1) perpendicular to the medial plane. The terminal floral meristem subsequently broadens in the lateral plane, resulting in a bilateral flattened plate (late floral stage 5). At floral stage 6, differential growth has resulted in a central invagination positioned along the lateral plane, and differential gene expressions indicate that initial patterning events distinguishing medial and lateral domains as well as inner (adaxial) and outer (abaxial) tissues have initiated (Bowman et al., 1999). By the end of floral stage 7, the adaxial medial tissues grow toward each other, forming two medial ridges, also called carpel margin meristems (CMMs). The CMMs will give rise to placentae and subsequently ovule primordia at floral stage 8 (Schneitz et al., 1995). By stage 9, the major tissue types of the mature gynoecium become morphologically distinct as the style and stigmatic papillae start to differentiate. Cell differentiation and cell expansion continue during stages 10 to 12, and the gynoecium is fully mature and ready to accept pollen approximately 10 d after it started to initiate from the terminal floral meristem.

It is commonly accepted that the plant hormone auxin is important for gynoecium development, and several models have been put forward to explain this on a mechanistic level (Nemhauser et al., 2000; Østergaard, 2009; Sundberg and Østergaard, 2009; Nole-Wilson et al., 2010; Marsch-Martínez et al., 2012; Hawkins and Liu, 2014). However, we still lack a clear picture of the auxin dynamics and response sites during the earliest developmental stages when the major patterning decisions are made. During lateral organ development, instructive auxin peaks or gradients are formed by site-specific auxin biosynthesis and polar auxin transport (PAT), which results in procambium formation, organ outgrowth, and tissue differentiation (Sachs, 1969; Benková et al., 2003; Mattsson et al., 2003; Heisler et al., 2005; Scarpella et al., 2006; Furutani et al., 2014). The plasma membrane-bound PINFORMED (PIN) proteins as well as at least four members of the ATP-binding cassette subfamily B (ABCB)/MULTI-DRUG RESISTANT/P-GLYCOPROTEIN (PGP) protein family show auxin efflux capacity (for review, see Habets and Offringa, 2014). The PIN proteins are often polarly localized at the plasma membrane, whereas the ABCB/PGP proteins are generally localized apolarly. Therefore, the PINs are largely responsible for the net directional flow of auxin, while the ABCB proteins most likely contribute to PAT by regulating the effective cellular auxin available for polar transport (Mravec et al., 2008; Wang et al., 2013). The phytotropin 1-*N*-naphtylphthalamic acid (NPA) is a well established and widely used PAT inhibitor, although its exact mode of action is obscure (Petrásek et al., 2003). NPA treatment mimics the pin-like shoot phenotype of *pin1* loss-of-function mutants (Okada et al., 1991), and even though NPA appears not to directly interact with PIN proteins, it may influence subcellular dynamics and has been shown to bind to ABCB family members, thereby blocking their transport capacity (Noh et al., 2001; Murphy et al., 2002; Geisler et al., 2003; Nagashima et al., 2008; Kim et al., 2010). This suggests that NPA

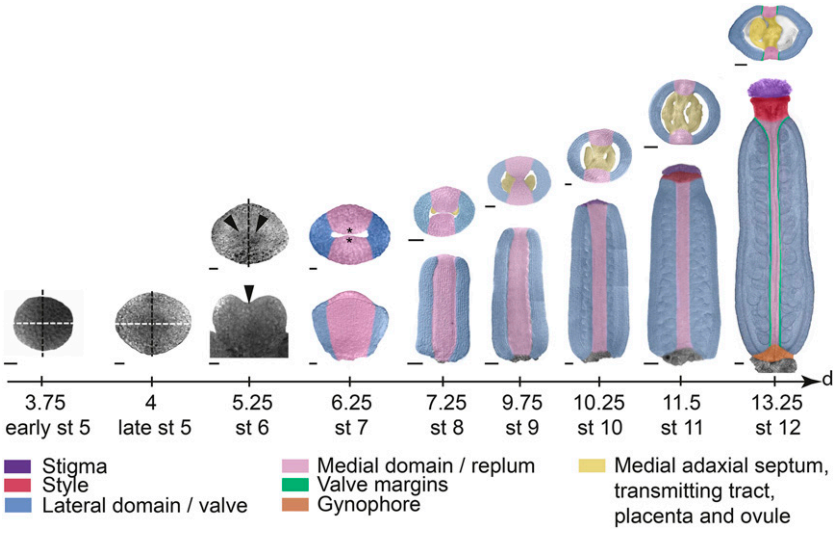

Figure 1. Arabidopsis gynoecium development. Transmitted light confocal images of the remaining floral meristem (stage [st] 5) and the first stages of gynoecial primordia development (stages 6 and 7), and false-colored DIC images of floral stages 8 to 12 gynoecia along a developmental time scale showing the time in days after floral initiation at the end of each stage. Early and late stage 5 as well as upper images at floral stages 6 and 7 are viewed from above. Lower floral stage 6 image is viewed from the lateral side. Lower images of floral stages 7 to 12 gynoecia are viewed from the medial side. Upper images of floral stages 8 to 12 gynoecia show transverse sections. Stages and time scale are adapted after Smyth et al. (1990) and Sessions (1997). White dashed lines indicate lateral plane, black dashed lines indicate medial plane, arrowheads indicate lateral crease, and asterisks indicate CMM. Bars = 10 μm (stages 5–7), 25 μm (stages 8–10), and 50 μm (stages 11 and 12).

may reduce PAT in part by restricting the amount of auxin available for PIN-mediated polar transport.

Although the *pin1-1* knockout mutant rarely produces flowers (Okada et al., 1991), gynoecia of the hypomorphic *pin1-5* mutant form elongated styles and reduced or even missing carpels (Bennett et al., 1995; Sohlberg et al., 2006). Auxin biosynthesis mutants also produce disproportionate gynoecial tissues (Cheng et al., 2006; Stepanova et al., 2008), suggesting that auxin peaks and fluxes are important for the coordinated development of gynoecial domains. However, because the gynoecium is the last organ to initiate from the floral meristem, the abnormal gynoecial development in auxin-related mutants may result from developmental defects that occurred prior to gynoecium formation. By transiently treating inflorescences with NPA, Nemhauser et al. (2000) showed that PAT in the gynoecial primordia is important for differential development. However, the whole gynoecium was regarded as one entity with apical-basal polarity, and the possibility that the lateral carpels and the medial meristematic tissues could respond differently to the treatment was never discussed. Thus, where and how NPA affects PAT-regulated development has remained elusive.

To understand how local auxin activities influence the outgrowth and patterning events of young gynoecial primordia, we determined the localization of PIN and PGP auxin efflux proteins and the resulting auxin response domains. This allowed us to map the directional flow and auxin response peaks during the earliest stages of gynoecium development. In addition, we induced transient disruptions in PAT and assessed the response of auxin signaling and domain-specific markers to establish how auxin signaling and vascular, lateral, and medial domains are affected by alterations in PAT. Based on our data, we propose a new model for auxin-regulated gynoecial patterning in which the medial versus lateral identity is dependent on correct auxin localization, and subsequent carpel valve outgrowth is dependent on transport-mediated apical auxin drainage.

RESULTS

Carpel Primordia Initiation Correlates with Acropetal and Bilateral Auxin Transport as Well as Bilateral Auxin Responses

To determine the flow of auxin during the earliest stages of gynoecium development, we analyzed the localization of the plasma membrane-bound PINs (PIN1–PIN4 and PIN7) using translational reporters and compared these with the activity of the synthetic auxin response element promoter, referred to as *DR5* (Ulmasov et al., 1997). The $PIN1_{pro}$:*PIN1-GFP* reporter (Benková et al., 2003) is expressed throughout gynoecium development, and both $PIN3_{pro}$:*PIN3-GFP* (Zádníková et al., 2010) and $PIN7_{pro}$:*PIN7-GFP* (Blilou et al., 2005) reporters showed transient but conspicuous expression patterns, whereas no PIN2 or PIN4 reporter activity was detected in developing gynoecia. At early floral stage 5 (Fig. 2A), PIN1 is expressed in the entire periphery of the remaining floral meristem in the L1 cell layer and is localized to the apical plasma membrane, presumably pumping auxin toward the tip of the incipient gynoecial primordium (Fig. 2B). In accordance, the auxin response reporter *DR5rev*:*3xVENUS-N7* (Heisler et al., 2005; Vernoux et al., 2011) is expressed in a band along the lateral plane of the terminal meristem (Fig. 2C). An identical expression pattern was seen with the *DR5rev*:*GFP* reporter (Friml et al., 2003; Supplemental Fig. S1). As the dome-shaped floral meristem subsequently broadens in the lateral plane (late floral stage 5; Fig. 2E), PIN1 localization in the apical-most cell layer is shifted toward two convergence points (Fig. 2F), one in each lateral domain, which subsequently will give rise to the two carpel primordia. These convergence points were confirmed by a shift in *DR5* expression to two bilaterally localized foci (Fig. 2G). At floral stage 6 (Fig. 2I), PIN1 is continuously expressed in the surface cell layer (Fig. 2J) and *DR5* expression remains strong in the two lateral foci (Fig. 2K). In addition, we detected weak *DR5* expression in the apical-most cell layer of the medial domains in 66% of the gynoecial primordia examined. At this stage, strong $PIN3_{pro}$:*PIN3-GFP* activity was first detected in a few laterally positioned apical cells together with weaker expression in some surface cell files of the apical medial domain (Fig. 2M). PIN3 expression was also detected in the center of the gynoecial base (Supplemental Fig. S2A), and $PIN7_{pro}$:*PIN7-GFP* was transiently expressed in the basal medial domain at floral stages 6 and 7 (Supplemental Fig. S2B). In the internal cell layers of the lateral domains, PIN1 expression becomes confined to two regions (Fig. 2N) basal to the convergence points detected earlier (see Fig. 2F). These regions also showed strong *DR5* expression (Fig. 2O), whereas no subapical auxin response can be detected in the medial domains at this stage.

Together, our results suggest that already before the outgrowth of the gynoecium, auxin is actively transported to prepattern the lateral axis in the incipient primordium. Subsequently, active auxin transport restricts auxin responses to the apical centers of the two emerging carpels. The lack of PIN1 and *DR5* expression in the subapical medial tissues of early gynoecial primordia suggests that distinct auxin maxima are delayed in the medial domains relative to the lateral domains.

PIN Expression Differs between Medial and Lateral Domains

As the morphological differences between medial and lateral domains become more distinct at floral stage 7 (Fig. 3, A and B), a clear divergence in PIN1 expression appears (Fig. 3C). In the lateral domains, PIN1 is expressed and apically localized in the outer (Fig. 3D) and inner (Fig. 3E) epidermal cell layers. The internal cell layers are devoid of PIN1 expression, except for a few centrally positioned longitudinal cell files in which PIN1 is localized to the basal plasma membrane (Fig. 3F). By contrast, PIN1 is expressed across the medial domains from the outer to the inner epidermal cell layers, and

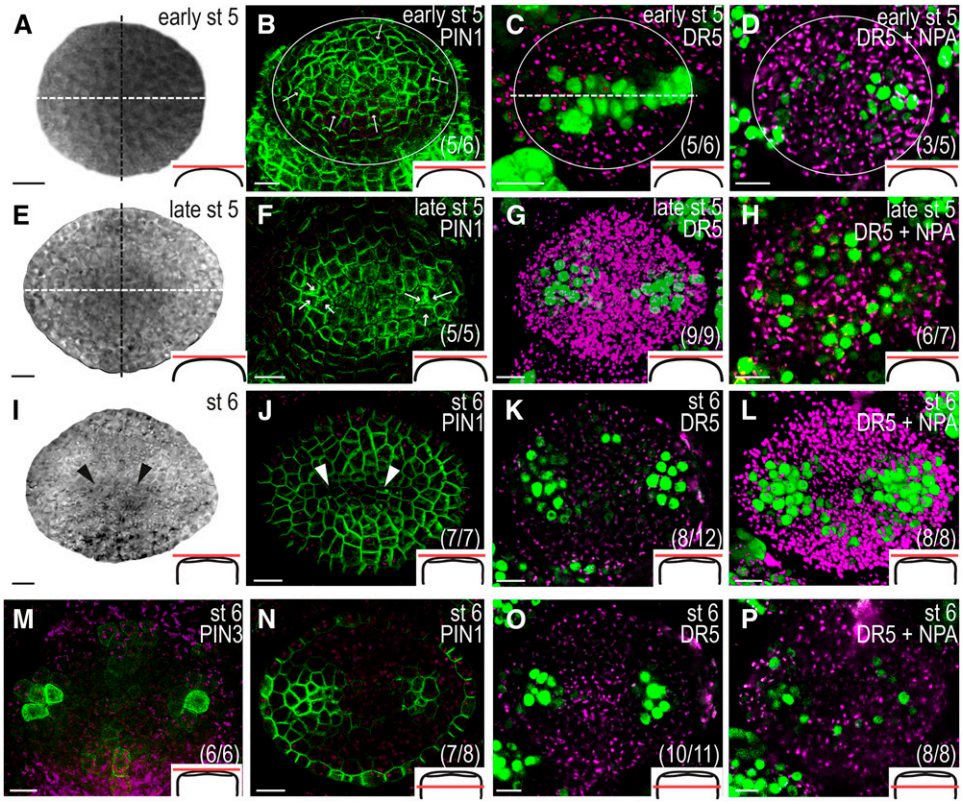

Figure 2. The localization of PIN protein and auxin response reporters is dynamic in the remaining floral meristem and early gynoecial primordia. Early floral stage (st) 5 (A–D), late floral stage 5 (E–H), and floral stage 6 (I–P). A, E, and I, Transmitted light confocal images of the remaining floral meristem and the first stages of gynoecial primordia development viewed from above. B, F, J, and N, PIN1 localization in the L1 cell layer of the meristem and gynoecial primordia viewed from above (B, F, and J) and approximately three cell layers below the apex (N). C, D, G, H, K, L, O, and P, *DR5rev:3xVENUS-N7* expression in mock-treated gynoecia (C, G, K, and O) and in gynoecia treated with NPA for 24 h (D, H, L, and P) seen from above (C, D, G, H, K, and L) and approximately three cell layers below the apex (O and P). M, PIN3 localization seen from above. Magenta indicates chlorophyll autofluorescence, circles indicate remaining floral meristem, white dashed lines indicate lateral plane, black dashed lines indicate medial plane, arrows indicate presumptive auxin transport, arrowheads indicate lateral crease, schematic drawings in bottom right corner indicate the tissue viewed in each image, and parentheses indicate fraction of primordia showing the displayed features. Bars = 10 μm.

although the localization in the outer epidermis is apical (Fig. 3G), PIN1 localization in the inner epidermis appears less polarized (Fig. 3H). In a number of central internal cell files, PIN1 is localized to both basal and lateral plasma membranes (Fig. 3I).

The stage 6 PIN3 expression pattern is maintained at stage 7, but it broadens and gets stronger (Fig. 3J). In the lateral domains, PIN3 is only expressed in the apical-most cell layer, while in the medial domains, PIN3 expression can be detected also in one or two subapical cell layers in the outer epidermal tissues (Fig. 3K) and in several cell layers of the inner epidermal tissues in which the expression gradually decreases from the apex to the base (Fig. 3L). In contrast to PIN1, PIN3 is not expressed throughout the medial domains. However, PIN3 localization overlaps with that of PIN1 in one or two medial internal cell files (Fig. 3M).

Together, the PIN localization data suggest that auxin has a distinct transport route in the lateral domains, directing auxin apically in inner and outer epidermal cell layers and basally in a few internal cell files.

Regulated PAT Marks the Lateral Preprocambia

Certain PIN localizations during early gynoecium development, particularly in the lateral domains, are reminiscent of those during preprocambium formation in young leaves (Mattsson et al., 2003; Scarpella et al., 2006). In mature gynoecia (floral stage 12), four main vascular strands (one in each replum and one in each carpel) run along the apical-basal axis, and the differentiation of these strands begins at stage 8 (Sessions, 1997). The PIN localization in internal cell files at floral stage 7 continues to coincide with strong *DR5* activity in the lateral domains and weaker *DR5* activity in the medial domains (Fig. 4, A and C), suggesting that PIN and *DR5* expression mark preprocambium initiation sites

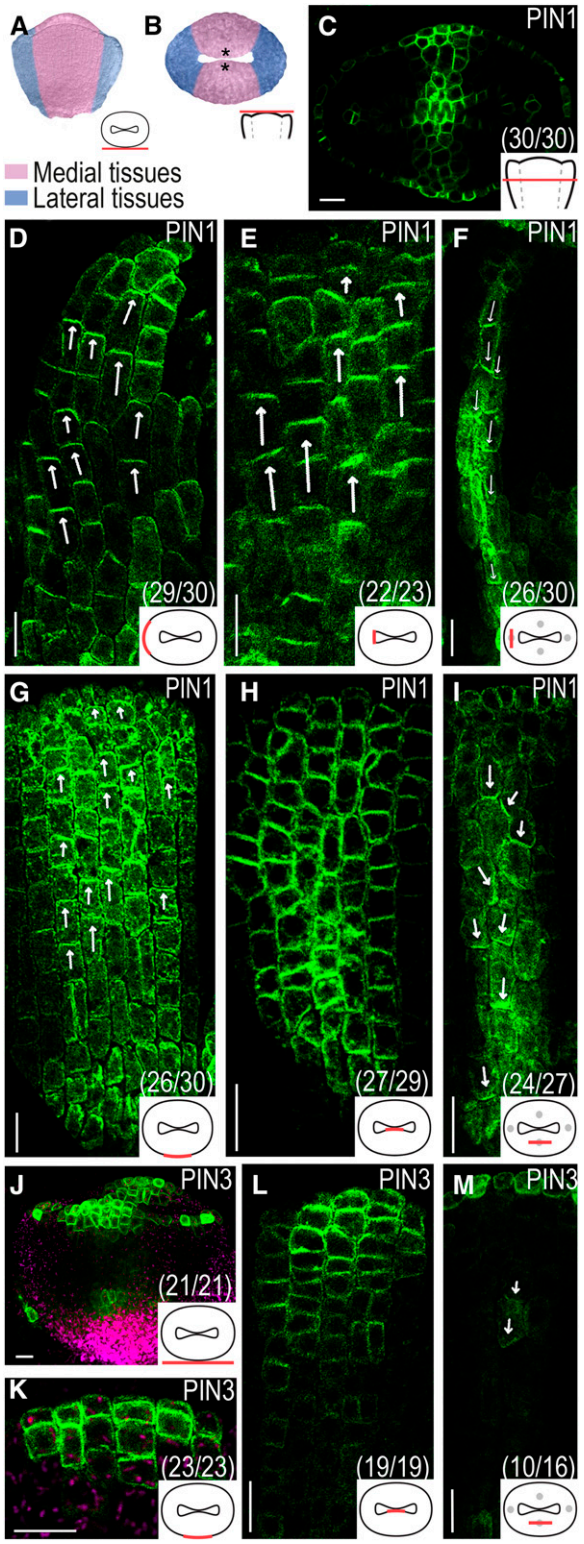

Figure 3. PIN localization in gynoecial primordia at floral stage 7. A and B, False-colored stage 7 gynoecial primordia viewed from the medial side (A) and viewed from above (B). C to I, PIN1 localization seen in an optical transverse section (C), in optical longitudinal sections of the lateral domain (D–F), and in optical longitudinal sections of the medial domain (G–I). J to M, PIN3 localization viewed from the medial side (J) and in optical longitudinal sections of the medial domain (K–M). Magenta indicates chlorophyll autofluorescence, asterisks indicate CMM, arrows indicate presumptive auxin transport, schematic drawings in bottom right corner indicate the tissue viewed in each image, and parentheses indicate fraction of primordia showing the displayed features. Bars = 10 μm.

in the gynoecial primordium. To test this hypothesis, we analyzed the expression domain of the *AUXIN/INDOLE-3-ACETIC ACID* (*IAA*) gene *IAA2* using an $IAA2_{pro}$:*GFP* reporter construct that has been used as an auxin-induced vascular marker in roots (Bishopp et al., 2011). $IAA2_{pro}$:*GFP* expression could be detected already at floral stage 5 (Fig. 4E) and is, at this and later stages, confined to the same lateral foci as *DR5*, PIN1, and PIN3 (Fig. 4, G and I). This suggests that the lateral preprocambia are specified already in the congenitally fused carpel primordium. In comparison, the appearance of $IAA2_{pro}$:*GFP* expression in the medial domains was delayed and could not be detected until late stage 7 or early stage 8 (Fig. 4K). This medial delay is similar to that observed with the *DR5* reporter, which becomes clearly expressed in the presumptive medial preprocambia starting at stage 8 (Fig. 4L).

PIN3 Marks Ovule Primordia Initiation and Incipient Style and Stigma Development

As the placentae are formed during stage 8 (Fig. 5A), PIN3 is expressed in clusters of a few cells in the adaxial medial domains (Fig. 5, B–D), most likely marking the initiation of ovules at these sites. In accordance, ovule primordia are marked by *DR5* as they grow out (Benková et al., 2003). From late stage 7/early stage 8, PIN3 is expressed in apical cells all around the gynoecium apex (Fig. 5E), where it coincides with *DR5* activity at late stage 8/early stage 9, just before the first stigmatic papillae become visible and the apical tissues fuse to form the style (Fig. 5F; Larsson et al., 2013). This suggests that directed auxin transport and auxin responses mark tissue specification and differentiation throughout gynoecium development.

Disruption of Polar Auxin Transport Alters the Auxin Response Domains, Preprocambium Formation, and Domain Specification in the Gynoecial Primordium

To test the role of PAT in the formation of auxin response sites during early gynoecium development, we treated inflorescences of various auxin-related and domain-specific reporter lines with the PAT inhibitor NPA as described by Nemhauser et al. (2000). As flowers are iteratively produced from the inflorescence meristem, the Arabidopsis inflorescence contains a developmental series of flowers spanning all developmental stages, and therefore flowers of all developmental stages were treated with NPA at the same time. However, because the flowers develop with a predictable time course (see Fig. 1), we can,

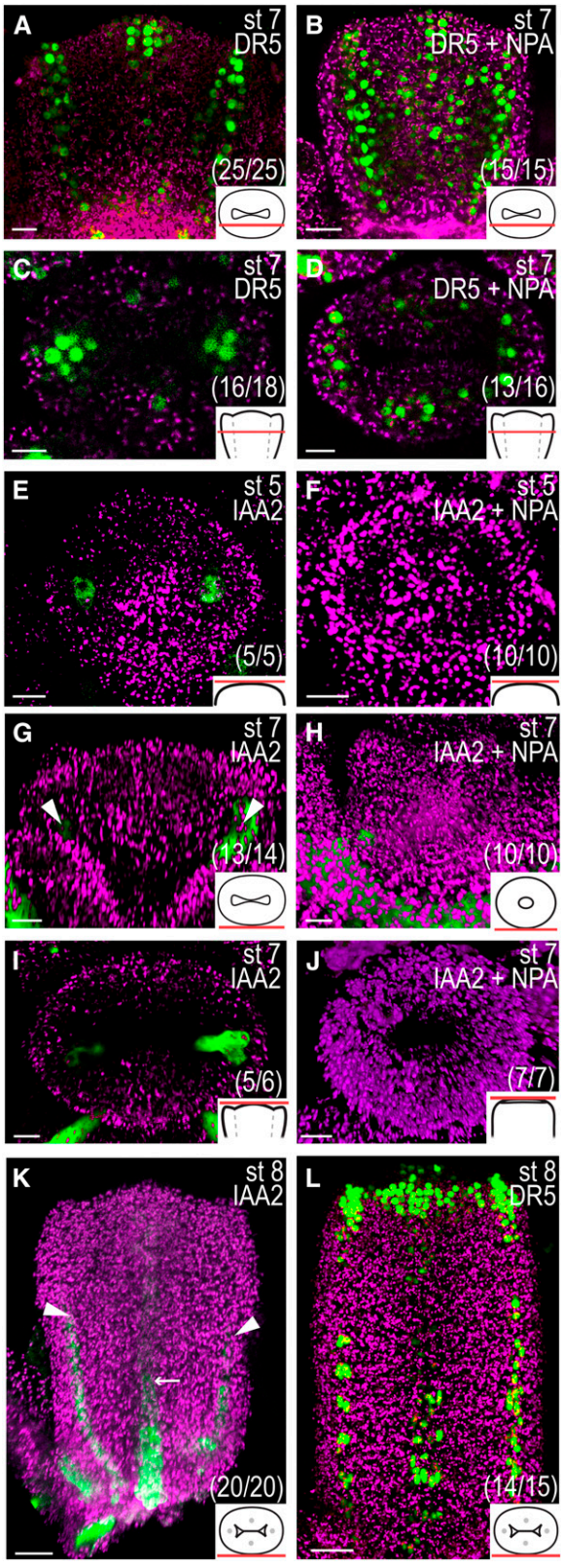

Figure 4. Auxin prepatterns vascular differentiation. A to D and L, *DR5rev:3xVENUS-N7* expression in optical longitudinal (A and B) and transverse (C and D) sections of floral stage (st) 7 mock-treated gynoecia (A and C) and gynoecia treated with NPA for 24 h (B and D) and in a mock-treated stage 8 gynoecium viewed from the medial side (L). E to K, $IAA2_{pro}$*:GFP* expression in mock-treated (E, G, and I) stage 5 (E) and stage 7 (G and I) gynoecia viewed from above (E and I) and from the medial side (G), in stage 5 (F) and stage 7 (H and J) gynoecia treated with NPA 72 h earlier viewed from above (F and J) and from the medial side (H), and in a mock-treated early stage 8 gynoecium viewed form the medial side (K). Magenta indicates chlorophyll autofluorescence, arrowheads indicate presumptive lateral preprocambium; arrows indicate presumptive medial preprocambium, schematic drawings in bottom right corner indicate the tissue viewed in each image, and parentheses indicate fraction of primordia showing the displayed features. Bars = 10 μm (A–J) and 50 μm (K and L).

assuming that NPA treatment does not dramatically alter the rate of development, estimate the stage of the flower at the time of treatment using the stage of the flower at the time of observation and the elapsed time between treatment and observation. Thus, the treatment stages listed here represent our best estimate of the floral stage at the time of treatment. Alterations in *DR5* activity could be detected already 7 h after NPA treatment (Supplemental Fig. S3, A and B) and became strong and consistent after 24 h (Figs. 2, D, H, L, and P, and 4, B and D). In early and late stage 5 floral meristems developing in buds that were NPA treated at floral stages 3 to 4, *DR5* was ectopically expressed and not confined to the lateral plane (compare Fig. 2C with Fig. 2D) or to two bilateral foci (compare Fig. 2G with Fig. 2H) as in mock-treated plants. In flowers treated with NPA after floral stage 5, at which point the apical auxin response foci have already been established, the *DR5* expression in this domain was less altered compared with after NPA treatments at earlier stages (compare Fig. 2K with Fig. 2L and Fig. 4A with Fig. 4B). Still, NPA treatment after floral stage 5 induced *DR5* activity outside the single internal cell files that were observed in mock-treated gynoecial primordia (compare Fig. 2O with Fig. 2P, Fig. 4A with Fig. 4B, and Fig. 4C with Fig. 4D), suggesting that canalized auxin drainage does not occur. NPA-induced ectopic *DR5* expression was detected 24 h after treatment in all developmental stages up until anthesis (Supplemental Fig. S3C). At later stages, particularly strong expression could be detected in the adaxial cell layers of the valves and in tissues adaxial to the replum vasculature (Supplemental Fig. S3D).

Clear morphological abnormalities could be detected in gynoecial primordia 72 h after NPA treatment. Stage 6 and 7 gynoecia treated with NPA at floral stages 3 to 4 displayed a doughnut-shaped morphology when viewed from above (Figs. 4J and 6, C, E, I, K, O, and Q). These gynoecia did not exhibit distinct morphological differences between medial and lateral domains and fail to form medial ridges. Doughnut-shaped gynoecia completely lacked detectable $IAA2_{pro}$*:GFP* expression, which instead was restricted to the receptacle below the developing gynoecium and to the outer floral organs (compare Fig. 4, F, H, and J, with Fig. 4, E, G, and I). This suggests that NPA treatment interferes with

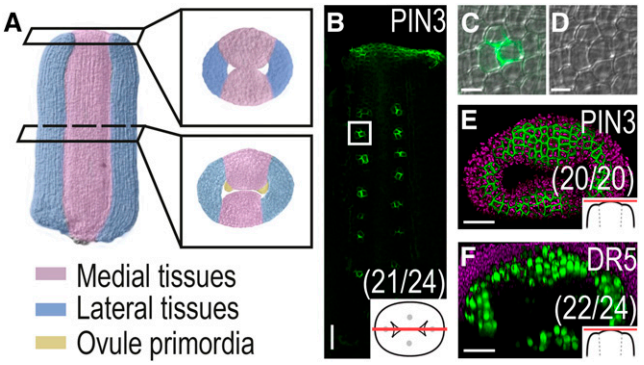

Figure 5. Auxin marks ovule differentiation as well as style and stigma formation. A, False-colored gynoecium at late floral stage 8 showing lateral and medial tissues with placentae primordia. B to D, Optical longitudinal section showing PIN3 expression in placentae or ovule primordia at floral stage 8. Square in B indicates enlarged section shown in C with PIN3 expression and in D without PIN3 expression. E and F, PIN3 (E) and *DR5rev*::*3xVENUS-N7* expression (F) in gynoecia at floral stage 8 viewed from above. Magenta indicates chlorophyll autofluorescence, schematic drawings in bottom right corner indicate the tissue viewed, and parentheses indicate fraction of gynoecia showing the displayed features. Bars = 5 μm (C and D) and 20 μm (B, E, and F).

lateral preprocambium formation in young gynoecial primordia.

The effects of PAT disruption on mediolateral tissue specification were studied using reporter lines of genes expressed in either medial or lateral domains during early gynoecium development. The auxin biosynthesis gene *TRYPTOPHAN AMINOTRANSFERASE OF ARABIDOPSIS1* (*TAA1*) is expressed in the adaxial medial domains of young gynoecia (Stepanova et al., 2008), and *SHATTERPROOF2* (*SHP2*) is expressed in the medial tissues of gynoecia up to floral stage 9 (Dinneny et al., 2005). By contrast, the *FILAMENTOUS FLOWER* reporter line FIL_{pro}:*GFP* is specifically expressed in the lateral domains (Watanabe and Okada, 2003). We observed that $TAA1_{pro}$:*GFP-TAA1* (Stepanova et al., 2008) is expressed throughout early floral stage 5 meristems (Fig. 6A), and it is not until after the transition from radial to bilateral symmetry that the *TAA1* activity becomes gradually restricted to the adaxial portions of the medial domains (Fig. 6, B and D). The restriction of *TAA1* expression to the medial domains fails in the doughnut-shaped, NPA-treated gynoecia, resulting in an ectopic expansion all around the internal gynoecial cavity at floral stages 6 to 7 (compare Fig. 6B with Fig. 6C and Fig. 6D with Fig. 6E). The difference in expression pattern between mock- and NPA-treated gynoecial primordia is unlikely to be a direct effect of increased auxin levels at atypical sites, because no difference in the $TAA1_{pro}$:*GFP-TAA1* expression pattern can be detected at 24 or 48 h after treatment (i.e. before morphological abnormalities are observed). The *SHP2* promoter activity was studied using a two-component system based on the *SHP2* promoter fused to the sequence encoding the transcriptional activator GAL4 ($SHP2_{pro}$:*GAL4*) driving an *Upstream Activation Sequence* fused to three copies of the sequence encoding YELLOW FLUORESCENT PROTEIN (A. Stepanova, J. Alonso, J. Brumos, and L. Robles, unpublished data), hereafter referred to as $SHP2_{pro}$ >>*YFP*. This reporter was weakly active in the abaxial portions of the medial domains of incipient gynoecial primordia from floral stage 5 (Fig. 6G). The expression intensified at stage 6 (Fig. 6H) and marked the whole medial domains at floral stage 7 (Fig. 6J). In accordance with the *TAA1* reporter, *SHP2* expression becomes ectopic in doughnut-shaped, NPA-treated gynoecia so that *SHP* expression can be detected throughout the abaxial domain of gynoecial primordia at floral stage 6 (Fig. 6I) and around the whole apical part of the gynoecium at floral stage 7 (Fig. 6K). In mock-treated floral buds, faint activity of the FIL_{pro}:*GFP* reporter could be detected in the subapical cell layers of the lateral domains in late floral stage 5 meristems (Fig. 6M), and the expression remained strictly confined to the valves throughout development (Figs. 6, N, P, and R, and 7A). In approximately one-third of the doughnut-shaped, NPA-treated gynoecia, *FIL* expression was strongly reduced or restricted to only one of the lateral domains (Fig. 6, O and Q). The expansion of medial marker expression into the lateral domains and the reduction of lateral marker activity suggest that PAT disruption interferes with the establishment of lateral identity during the transition from floral meristem to gynoecial promordium that occurs during floral stage 5.

Failure to Establish Boundaries between Medial and Lateral Domains in the Gynoecial Primordium Affects the Ratio between Medial and Lateral Tissues in the Mature Gynoecium

Previous reports describing the effects of NPA on gynoecial morphology have mainly focused on the enhanced growth of the style, stigma, and gynophore at the expense of ovary growth (Nemhauser et al., 2000; Sohlberg et al., 2006; Ståldal et al., 2008). Two weeks after NPA treatment, we observed the same frequency of reduced valves, very reduced valves, and valveless phenotypes as reported previously (Sohlberg et al., 2006). However, we also found that these apical-basal phenotypes are equally correlated to an asymmetric distribution of medial and lateral domains. Changes in the valve-specific reporter FIL_{pro}:*GFP* indicate that lateral tissues are reduced in both length and width, while medial tissues appear to be unaffected (Fig. 7, A–C and J–L.). Transverse sections of the reporter line revealed that cell fates along the mediolateral axis are altered in NPA-treated gynoecia such that either only one valve is detected (Fig. 7K) or one valve is enlarged, while the second valve, consisting of only a few cell files, is positioned opposite to the larger valve (compare Supplemental Fig. S4A with Fig. 7J). Furthermore, the medial tissues are delocalized and produce fewer or no ovules (Fig. 7, K, N, and Q). Using $SHP2_{pro}$ >>*YFP* as a valve margin marker in mature gynoecia (Fig. 7, D–F and M–O; Roeder et al., 2003), we found that NPA treatment shifts *SHP2*

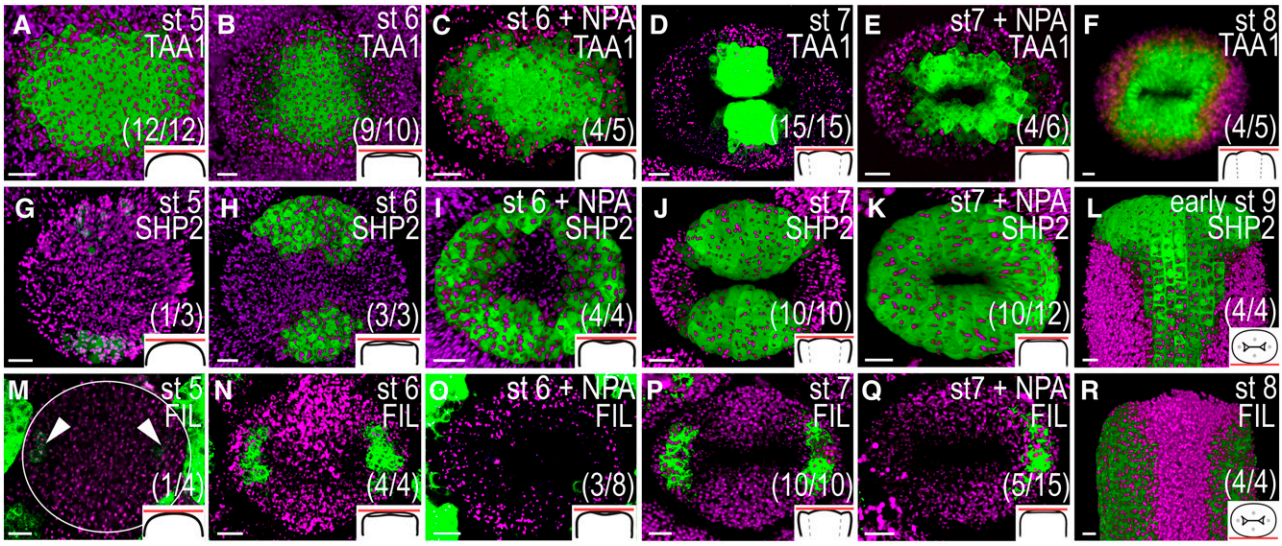

Figure 6. Domain-specific gene expression patterns are altered in young gynoecia 72 h after NPA treatment. A to F, $TAA1_{pro}$:*GFP-TAA1* expression in mock-treated (A, B, D, and F) and NPA-treated (C and E) remaining floral meristems and gynoecia viewed from above. G to L, $SHP2_{pro}$:*YFP* expression in mock-treated (G, H, J, and L) and NPA-treated (I and K) gynoecia viewed from above (G–K) and from the medial side (L). M to R, FIL_{pro}:*GFP* expression in mock-treated (M, N, P, and R) and NPA-treated (O and Q) gynoecia viewed from above (M–Q) and from the medial side (R). A, G, and M, Floral stage (st) 5. B, C, H, I, N, and O, Floral stage 6. D, E, J, K, P, and Q, Floral stage 7. F and R, Floral stage 8. L, Early floral stage 9. Magenta indicates chlorophyll autofluorescence, circles indicate remaining floral meristem; arrowheads indicate lateral *FIL* expression, schematic drawings in bottom right corner indicate the tissue viewed, and parentheses indicate fraction of gynoecia showing the displayed features. Bars = 10 μm.

expression along the mediolateral axis such that sometimes only two or three *SHP2*-expressing domains are found, instead of four as in mock-treated gynoecia (compare Fig. 7N and Supplemental Fig. S4B with Fig. 7M). A shift in medial versus lateral tissue identity is further confirmed by the expression patterns of the *KNOTTED-like from Arabidopsis thaliana1* reporter, $KNAT1_{pro}$:*GUS* reporter (Ori et al., 2000), whose activity is restricted to the replum (Fig. 7, G and P). In NPA-treated gynoecia, $KNAT1_{pro}$:*GUS* expression was spread out such that it covered about one-third of the tissues in gynoecia that appear to have only one valve (Fig. 7, H and Q). On average, one gynoecium per inflorescence appeared rod shaped 2 weeks after NPA treatment, as it completely lacks an ovary or has an extremely small ovary (Fig. 7, C, F, and I). These gynoecia lacked FIL_{pro}:*GFP* activity (Fig. 7, C and L), and transverse sections reveal a striking similarity to the styles of mock-treated gynoecia (Fig. 7, L, O, and R, compare with insets). Just as in styles, *SHP2* is expressed in the central tissues of rod-shaped gynoecia (Fig. 7O and inset), and $KNAT1_{pro}$:*GUS* is expressed throughout the rod-shaped gynoecia (Fig. 7, I and R).

PGP Proteins Are Involved in the Establishment of Apical Auxin Response Maxima in the Lateral Domains

As PIN expression is not detected in the cells where the NPA-induced ectopic auxin responses are observed and as NPA has been shown to specifically bind to and block the function of the ABCB/PGP proteins PGP1 and PGP19 (Noh et al., 2001; Murphy et al., 2002; Nagashima et al., 2008; Kim et al., 2010), we analyzed the expression domains and possible roles of PGP1 and PGP19 during early gynoecium development. The plasma membrane localization of the fusion proteins expressed by the $PGP1_{pro}$:*PGP1-GFP* and $PGP19_{pro}$:*PGP19-GFP* constructs (Mravec et al., 2008) appeared mostly apolar in incipient and early gynoecial primordia (Fig. 8, A–H.). PGP1 was expressed in all cells at the analyzed developmental stages (Fig. 8, A–D), whereas PGP19 was differentially expressed. At floral stage 5, PGP19 expression was detected in the cells around the meristem periphery (Fig. 8E) and at floral stage 7, it was detected in most cell layers of the medial and lateral domains, except in the inner epidermis and the apical-most cell layers (Fig. 8, F–H). PGP1 and PGP19 were thus expressed outside of the PIN activity domain in several inner valve cells, which showed ectopic *DR5* activity after NPA treatment (compare with Fig. 4, B and D). By contrast, the medial tissue expression of PGP1, PGP19, and PIN1 largely overlapped, and NPA treatment led to ectopic *DR5* activity in cells expressing all three proteins in these domains.

We further assessed the gynoecial phenotype and *DR5* expression in the *pgp1 pgp19* double mutant (Noh et al., 2001). Because this mutant is in the Wassilewskija (Ws) ecotype, we used F3 plants from the cross between *DR5rev*:*GFP* (ecotype Columbia [Col-0]) and *pgp1 pgp19* (Ws), which expressed only wild-type *PGP1* and *PGP19* alleles as controls for all *pgp1 pgp19* experiments (hereafter referred to as the wild type). Although the

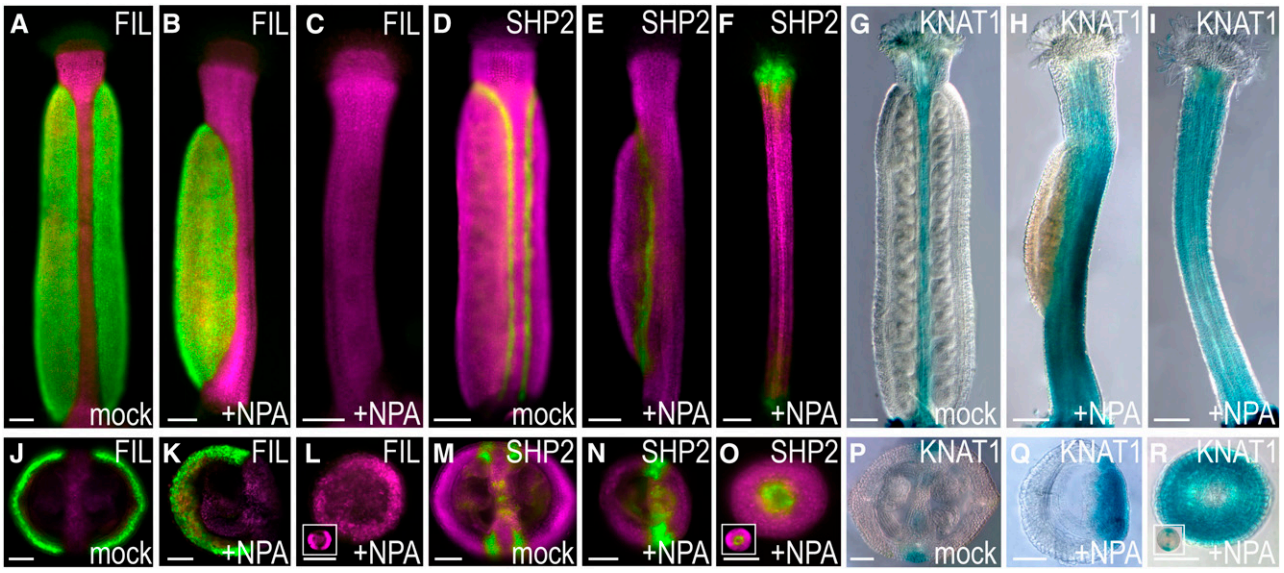

Figure 7. Domain-specific gene expression patterns are altered in mature gynoecia 2 weeks after NPA treatment. FIL_{pro}:*GFP* (A–C and J–L), $SHP2_{pro}$ >>*YFP* (D–F and M–O), and $KNAT1_{pro}$:*GUS* (G–I and P–R) expression in mock-treated (A, D, G, J, M, and P) and NPA-treated (B, C, E, F, H, I, K, L, N, O, Q, and R) gynoecia at floral stage 12. A to I, Longitudinal view; J to R, transverse sections. Inserts in L, O, and R show transverse sections of mock-treated style. Magenta indicates chlorophyll autofluorescence. Bars = 100 μm (A–I) and 50 μm (J–R).

pgp1 pgp19 mutant has severe vegetative defects (Noh et al., 2001; Geisler et al., 2005; Blakeslee et al., 2007; Mravec et al., 2008), the mature *pgp1 pgp19* gynoecium appeared morphologically similar to the wild type (Supplemental Fig. S5A). However, lateral, outer epidermal cells, and to a lesser extent the medial counterparts, developed in a less organized fashion with regards to cell division patterning and cell shape compared with the wild type (Supplemental Fig. S5, B and C). These results suggest that PGP1 and/or PGP19 are important for regulating the development of these tissues. As the *DR5rev*:*GFP* expression in the wild type is weak and variable at stages 5 to 6 and quite weak in the provascular domain below the apex in stages 7 to 8, likely the result of a generally weaker *DR5rev* signal in our Ws × Col-0 wild type compared with Col-0 (data not shown), we focused our analyses on the apical domain of stage 7 to 8 gynoecia where the *DR5rev* signal is strong. In the wild type, *DR5rev*:*GFP* was expressed in the apical-most cell layer of both medial and lateral domains in more than 90% of the observed gynoecia (Fig. 8, I and J). This is similar to what we see for the stronger *DR5rev*:*3xVENUS-N7* marker in Col-0 (compare with Fig. 4A). Although *DR5rev*:*GFP* activity could be detected in the apical-most cell layer of the medial tissues in 76% of the *pgp1 pgp19* stage 7 to 8 gynoecia (Fig. 8M), only 10% of these gynoecia showed a *DR5rev*::*GFP* signal in the apical-most cell layer of the lateral domains, while, instead, *DR5rev* expression was strongly detected in the subapical cell layers (Fig. 8, M and N). This suggests that PGP1 and/or PGP19 are required for the correct establishment of auxin signaling convergence points in the apex of the lateral domains.

To test if the NPA responsiveness in the *pgp1 pgp19* mutant is affected during gynoecial development, we studied the auxin response in the apical domain 24 h after NPA treatment. Although a strong and ectopic increase in *DR5rev*:*GFP* was observed in the apical part of wild-type gynoecia (Fig. 8L), a majority of stage 7 to 8 *pgp1 pgp19* gynoecia (72%) did not express ectopic *DR5rev*:*GFP* in the apex after NPA treatment (Fig. 8P). Instead, ectopic *DR5* expression was observed in the valves below the apex in 57% of the *pgp1 pgp19* gynoecia (Fig. 8O), compared with 12% in the wild type (data not shown). Two weeks after NPA treatment, only minor differences in developmental defects between the wild type and the *pgp1 pgp19* mutant were detected. Both *pgp1 pgp19* and wild-type gynoecia formed reduced and very reduced valves to a similar extent (Supplemental Fig. S6). However, while 11% of wild-type gynoecia were rod shaped, no rod-shaped gynoecia could be detected in *pgp1 pgp19* mutants, indicating that *pgp1 pgp19* mutants are slightly less sensitive to NPA. Our data thus suggest that PGP1 and PGP19 are involved in the establishment of the apical flow of auxin to the apices of the lateral domains but that inhibition of these two genes alone is not sufficient to dramatically block PAT during early gynoecium development.

DISCUSSION

The cellular and molecular complexity of the gynoecium and the position of the gynoecial primordium in enclosed floral buds have hindered our understanding of the earliest processes regulating gynoecial development. Here, we have assessed the flow of auxin and the

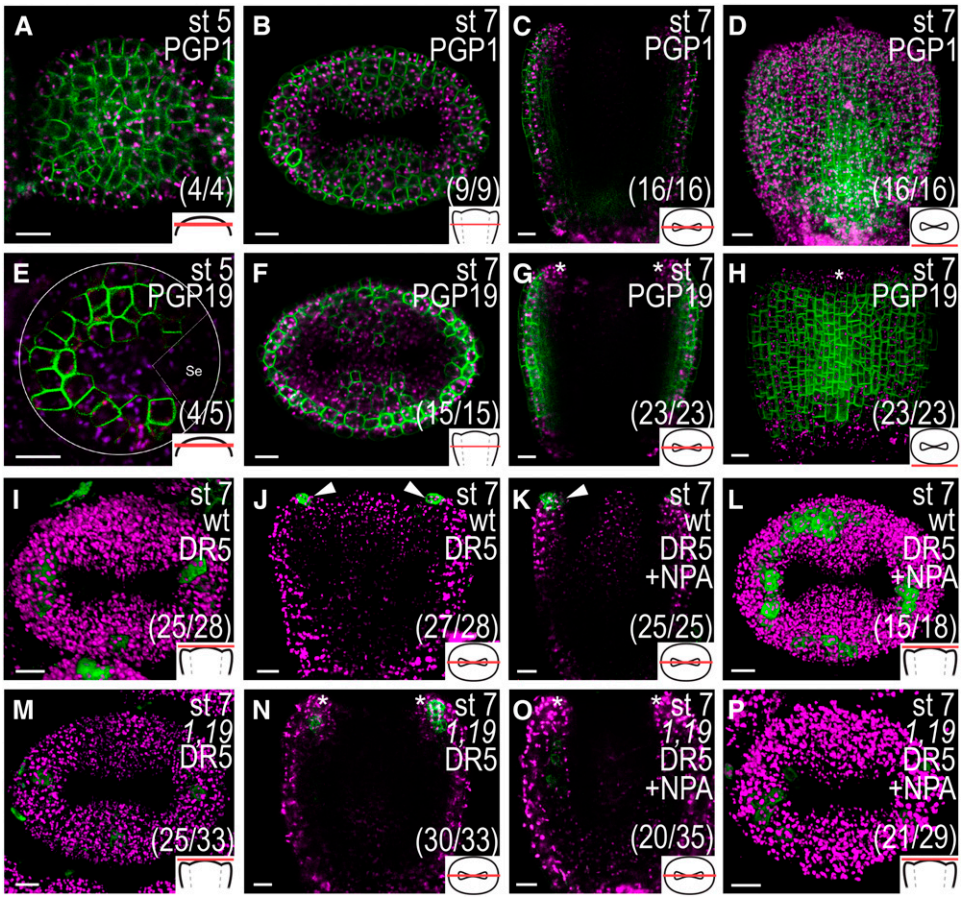

Figure 8. PGP1 and/or PGP19 are important for the formation of apical auxin response maxima. A to D, *PGP1pro:PGP1-GFP* expression in optical transverse sections of a stage (st) 5 remaining floral meristem (A) and stage 7 gynoecium (B) and an optical longitudinal section (C) and a three-dimensional reconstruction of a series of z-stack images (D) of a stage 7 gynoecium. E to H, *PGP19pro:PGP19-GFP* expression in optical transverse sections of a stage 5 remaining floral meristem (white circles; E) and a stage 7 gynoecium (F) and an optical longitudinal section (G) and three-dimensional reconstruction of a series of z-stack images (H) of a stage 7 gynoecium. A sepal partly covering the primordium in E is indicated by dashed lines and Se. I to L, *DR5rev:GFP* expression in wild-type (wt) stage 7 gynoecia viewed from above (I and L) and in longitudinal optical sections (J and K) 24 h after mock (I and J) or NPA treatment (K and L). M to P, *DR5rev:GFP* expression in *pgp1 pgp19* (1,19) double mutant stage 7 gynoecia viewed from above (M and P) and in longitudinal optical sections (N and O) 24 h after mock (M and N) or NPA treatment (O and P). Asterisks indicate lack of expression in the apical-most cell layer, arrowheads indicate expression in the apical-most cell layer, magenta indicates chlorophyll autofluorescence, schematic drawings in bottom right corner indicate the tissue type viewed, and parentheses indicate fraction of gynoecia showing the displayed features. Bars = 10 μm.

importance of auxin response maxima in patterning, differentiation, and growth of the gynoecium. We have utilized reporters for auxin response and PIN and PGP protein expression and localization, as well as for gynoecial domain specificity, to examine the role of auxin during the earliest stages of gynoecium development. Furthermore, we have examined early changes to auxin homeostasis brought about by transient NPA application and its effects on the establishment of tissue borders, differentiation, and growth. Thus, we present what we believe is the most comprehensive study to date on the role of auxin during early gynoecial patterning. We demonstrate that the flow of auxin differs between medial and lateral domains and that the lateral domains are more sensitive to NPA treatment. Early disruption of PAT results in a reprogramming of the developmental fate of the lateral domains, and the outgrowth of these domains is dependent on auxin drainage from the apex through the developing preprocambia. Based on our findings, we propose a new model for the role of auxin during early gynoecium patterning that will serve as a foundation for future studies on gynoecial development and on intertissue-specific communication.

The Initiation of Gynoecial and Carpel Primordia Is Marked by Auxin Maxima, and the Specification of Mediolateral Positional Identities Is Dependent on PAT

A PIN-mediated local auxin response maximum at the organ initiation site is required for the formation of

new lateral organ primordia at the flank of the shoot apical meristem (SAM; Benková et al., 2003; Reinhardt et al., 2003). In accordance, we detected an auxin response maximum along the lateral plane of the remaining floral meristem at early floral stage 5, which we propose may result from PIN1-directed apical flow of auxin produced throughout the meristem by *TAA1*-mediated auxin biosynthesis. Upon lateral primordium expansion, PIN1, and to some extent PIN3, redirects auxin toward the apical centers of the two lateral domains, corresponding to two congenitally fused incipient carpel primordia. This suggests that the initiation of the female reproductive organ follows the same principles as the initiation of other aerial lateral organs, except that it is divided into two steps, first initiating the whole organ primordium and subsequently defining the two lateral carpel primordia. At this early stage, PIN1-mediated PAT is also required for the specification of cellular identities across the mediolateral plane. NPA treatment results in expansion of medial marker expression (*SHP2* and *TAA1*) throughout the primordial region and a reduction in activity of the lateral marker *FIL*, suggesting that PAT is important for the establishment of lateral identity. Previous studies have revealed mutually antagonistic interactions between the lateral identity factors FIL, JAGGED, and ASYMMETRIC LEAVES (AS) and medial factors such as KNAT1 during gynoecium development (Dinneny et al., 2005; Alonso-Cantabrana et al., 2007; González-Reig et al., 2012). However, what activates the differential expression of these factors has remained elusive. Recent studies have shown that prolonged treatment of gynoecia with the plant hormone cytokinin causes the formation of reduced valves and valveless gynoecia (Zúñiga-Mayo et al., 2014), suggesting that both auxin and cytokinin are involved in the mediolateral patterning of the gynoecium. In the SAM, *SHOOT MERISTEMLESS* (*STM*) maintains meristem activity partially through induction of cytokinin biosynthesis (Yanai et al., 2005). During leaf initiation, PIN1-mediated auxin response maxima act together with AS1 to repress *KNAT1* and *STM* as well as cytokinin biosynthesis in incipient leaf primordia, thereby allowing leaf primordial outgrowth (Hay et al., 2006; Su et al., 2011). Here, we show that auxin regulates patterning along the mediolateral axis of incipient gynoecial primordia and restricts meristematic factors, such as KNAT1, to the medial domain. Thus, our data, together with the data from Zúñiga-Mayo et al. (2014), suggest a similar regulation of the medial domains and the SAM, while the lateral domains are initiated as lateral organs and need high auxin and low cytokinin for their outgrowth.

Apical Auxin Drainage and Early Preprocambium Formation

PIN1 and auxin response reporter expression patterns indicate that during early gynoecium development, auxin is transported according to the reverse fountain model (Benková et al., 2003) and that the apical part of both lateral and medial domains is provided with auxin from the base. Auxin is then drained from the apex through the preprocambium by canalized PIN1 expression, in line with the canalization hypothesis (Sachs, 1969) and similar to the mode of auxin transport and response in developing leaves (Scarpella et al., 2006). Recently, Furutani et al. (2014) genetically uncoupled PIN1-mediated auxin flow to apical foci of lateral organ primordia from the PIN1-mediated internal drainage, which contributes to vascular formation. Using loss-of-function mutants of *MACCHI-BOU4* (*MAB4*) family members, which encode proteins involved in the regulation of PIN protein endocytosis, they could show that these genes are required only for the basipetal PIN1 localization into internal tissues of incipient organ primordia. As a result, auxin drainage is prevented and auxin accumulates extensively at the surface of organ primordia in *mab* mutants, allowing for proper phyllotactic patterning but preventing primordial outgrowth. In accordance, our data show that PAT inhibition reduces the growth of already-established lateral carpel primordia. As this coincides with the loss of apical *IAA2* expression, it suggests that blocked PAT in emerging gynoecia prevents primordial outgrowth by inhibiting auxin drainage-induced vascular formation. Recently, Hawkins and Liu (2014) suggested that auxin-mediated abaxial/adaxial polarity in the incipient gynoecial primordium also drives gynoecium outgrowth and development. Although more data are needed to confirm their hypothesis, our results do not preclude the possibility that the observed auxin fluxes could also be instructive for abaxial/adaxial patterning.

Initial Auxin Flow in the Medial Domain Differs from Lateral Organs

Although differentiated vasculature appears simultaneously in medial and lateral domains of the young gynoecium (Sessions, 1997), PIN, *DR5*, and *IAA2* expression occurs earlier and is more conspicuous in the lateral domains compared with the medial domains, suggesting that the lateral preprocambia are specified before the medial preprocambia. While the vascular specification in the lateral domains seems to be guided by apically localized auxin response maxima already by stage 5, the medial vascular specification appears to begin only after substantial growth of the gynoecial primordium, suggesting that the medial domain is not dependent on preprocambial formation for initial growth and may be one of the reasons why outgrowth of the medial domain is less PAT dependent. However, the medial vasculature, which consists of more cell files compared with the lateral vasculature, supports the placentae from late stage 8 (Sessions and Zambryski, 1995; Sessions, 1997; Bowman et al., 1999), and the formation of placentae and ovules is severely inhibited when PAT is blocked.

NPA-Induced Inhibition of PAT May Result in Reduced PGP-Mediated Auxin Delivery to PIN1-Expressing Valve Cells

Upon NPA treatment, the auxin response broadened and was much less confined to apical foci or to the

presumptive preprocambia than in mock-treated carpel primordia. Our data suggests that NPA treatment prevents auxin from the internal cell layers of the lateral domains to become available for PIN1-mediated apical transport in the surface cell layer. This results in reduced auxin transport to the apical end of the carpel primordia, and as a consequence, reduced apical auxin available for basal drainage in the center of the lateral domains. Interestingly, we also found that the auxin efflux proteins PGP1 and PGP19, whose activity can be blocked by a direct interaction with NPA (Murphy et al., 2002; Geisler et al., 2003; Nagashima et al., 2008; Kim et al., 2010), were expressed not only in epidermal cells of the valves together with PIN1, but also in subepidermal valve cell layers outside of the PIN1 domain. This suggests that NPA-mediated block of PGP function could potentially entrap auxin in the internal cell layers of the valves, making it largely unavailable for PIN1-mediated apical transport in the epidermal valve cells. By contrast, some degree of PIN1-mediated transport could still occur in the medial domains where both PGP and PIN expression domains overlap. In support of the hypothesis that PGPs would provide epidermal cells with auxin is the disorganized patterning and reduced elongation of epidermal cells of *pgp1 pgp19* mutant gynoecia. This phenotype is similar to the reported epidermal phenotypes of roots and hypocotyls lacking functional PGP1 and PGP19 proteins or a functional version of the PGP-interacting partner TWISTED DWARF1 (Geisler et al., 2003; Bailly et al., 2006; Geisler and Bailly, 2007; Wang et al., 2013). However, as the mediolateral patterning and domain outgrowth of *pgp1 pgp19* gynoecia appear to occur normally, it is difficult to fully understand the importance of PGP1 and PGP19 in the regulation of auxin flow during gynoecial primordium development. Before we know if additional *PGP* genes might be acting functionally redundantly with *PGP1* and *PGP19*, or if the loss of specific PGP proteins is compensated for by ectopic expression of

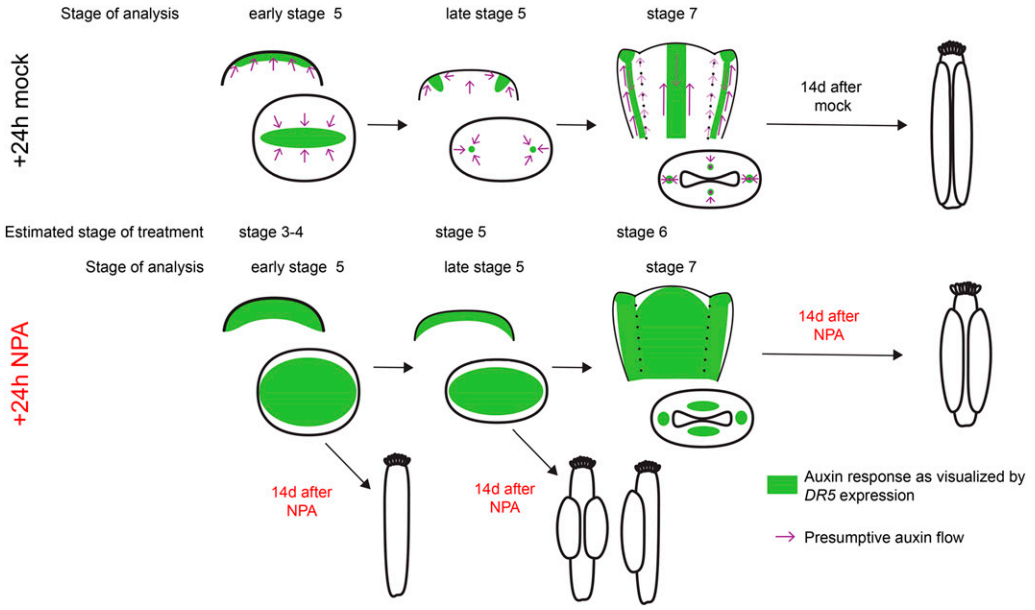

Figure 9. A model for the role of auxin during early gynoecial primordium development. Auxin is initially transported toward the remaining floral meristem (early floral stage 5), resulting in an auxin maximum along the lateral plane of the incipient gynoecial primordium. If PAT is blocked at this stage, the initial domain specification is altered, leading to the outgrowth of a rod-shaped gynoecium composed of cells predominantly expressing medial identity genes. This suggests that if auxin transport is perturbed before the two carpel primordia have been specified, valve outgrowth fails, while the medial tissues appear less affected. Just before the gynoecial cylinder starts to grow out from the floral meristem (late floral stage 5), PAT shifts toward two laterally localized foci. This creates convergence points and auxin response maxima in the centers of the two incipient carpel primordia that are essential for the subsequent auxin drainage down through the growing carpels. If PAT is reduced by transient NPA treatment at this stage, no clear lateral auxin maxima are established, leading to less canalized drainage through the growing tissues. This affects the outgrowth of the two lateral domains, which are dependent on auxin drainage at an earlier developmental stage compared with the medial domains, so that the valves are smaller and often developing only on one side of the gynoecium. Single-valved gynoecia most likely develop because of problems to establish two convergence points. At floral stage 7, both medial and lateral domains are provided with auxin from the base and dependent on auxin drainage through the procambium to grow. If PAT is reduced at this stage, canalization fails and auxin becomes trapped within the internal cell files of both medial and lateral domains, resulting in a broadened auxin response. Growth of the valves becomes repressed, most likely because of decreased procambial auxin drainage. The medial domains are less affected, perhaps because of the broad expression pattern of PIN1, which might still be able to translocate some auxin in these domains. Furthermore, NPA treatment stimulates precocious differentiation of stigmatic papillae, which previously has been shown to be induced by broadened apical auxin response maxima and therefore might result from the ectopic auxin responses caused by transiently affected PAT.

its homologs, which has been reported to occur for *PIN* genes in certain tissues (Vieten et al., 2005), we cannot conclusively say that they play a minor role during PAT-regulated gynoecium development.

CONCLUSION

To summarize our findings, we propose a model indicating the domains of auxin flow and accumulation and its effects on gynoecial primordium outgrowth (Fig. 9). In this model, we depict the effects of blocked PAT on both auxin response and gynoecial morphology. We suggest that the outgrowth of the lateral domains is dependent on lateral auxin response maxima and subsequent auxin drainage through the growing tissues. The medial tissues are less sensitive to perturbations in PAT, which may be explained by their meristematic characteristics and the broader PIN1 expression domain in the medial tissues compared with the lateral tissues as well as the later establishment of auxin response maxima and subsequent development of vasculature in these domains.

MATERIALS AND METHODS

Plant Material and Growth Conditions

Arabidopsis (*Arabidopsis thaliana*) Col-0 was used throughout this study unless otherwise stated. *DR5rev*:*3xVENUS-N7* (Heisler et al., 2005; Vernoux et al., 2011), *DR5rev*:*GFP* (Friml et al., 2003), $PIN1_{pro}$:*PIN1-GFP* (Benková et al., 2003), $PIN3_{pro}$:*PIN3-GFP* (Zádníková et al., 2010), $PIN7_{pro}$:*PIN7-GFP* (Blilou et al., 2005), $IAA2_{pro}$:*GFP* (Bishopp et al., 2011), $TAA1_{pro}$:*GFP-TAA1* (Stepanova et al., 2008), FIL_{pro}:*GFP* (Watanabe and Okada, 2003), $KNAT1_{pro}$:*GUS* (Ori et al., 2000), and $PGP1_{pro}$:*PGP1-GFP* and $PGP19_{pro}$:*PGP19-GFP* (Mravec et al., 2008) have been described before. $PGP1_{pro}$:*PGP1-GFP* and $PGP19_{pro}$:*PGP19-GFP* are in the *pgp1* and *pgp19* mutant background, respectively, and both are in the Ws. The *pgp1 pgp19 DR5rev*::*GFP* transgene was obtained by crossing *DR5rev*::*GFP* into the *pgp1 pgp19* mutant. The *pgp1* and *pgp19* alleles (Noh et al., 2001) were genotyped after performing DNA isolation by PCR using gene-specific and transfer DNA border primers. The gene-specific primer sequences used were PGP1 Fwd (5′-AAGCAGCTCACGAAACCGCCA-3′), PGP1 Rev (5′-CTGGGACCGGGGTGGTATCAGG-3′), PGP19 Fwd (5′-CCGATGCCAAGACTGTTCCAGCA-3′), and PGP19 Rev (5′-CCGGCGAAAGCGATTCCGGG-3′). The transfer DNA left border primer named JL-202 from the Wisconsin knockout facility (5′-CATTTTATAATAACGCTGCGGACATCTAC-3′) was used together with either the PGP1 Fwd or the PGP19 Rev primers to detect the presence of *pgp1* or *pgp19* alleles, respectively.

Plants were germinated on petri dishes with one-half-strength Murashige and Skoog medium supplemented with 1% (w/v) Suc and 0.8% (w/v) agar and then transplanted to soil and grown under controlled long-day growth conditions (16-h-light/8-h-dark photoperiod at 110 μmol m^{-2} s^{-1} and 22°C). For NPA treatments, flowering plants were sprayed both morning and afternoon with 100 μM NPA (Sigma-Aldrich) with 0.01% (v/v) Silwet L-77 as described by Nemhauser et al. (2000). NPA was dissolved in dimethyl sulfoxide to a stock concentration of 100 mM, and mock treatments were performed with distilled water containing 0.1% (v/v) dimethyl sulfoxide and 0.01% Silwet L-77. After 24 h of treatment, plants were sprayed with distilled water to wash away the treatment. Gene expression studies and morphologies were assessed continuously from 1 h after the first spray until 14 d after spraying.

Sample Preparations

Floral meristems and developing gynoecia were individually dissected from inflorescences and mounted in 0.3% (w/v) agarose (for confocal imaging), in water (for fluorescence microscopy), or in 30% (v/v) glycerol (for histochemical analysis).

For analysis of PIN localization, the inflorescences were fixed for 1 h in a solution containing 3.7% (v/v) paraformaldehyde, 50 mM PIPES, pH 6.8, 5 mM EGTA, 2 mM $MgSO_4$, and 0.4% (w/v) Triton X-100 (modified from Moschou et al., 2013). Fixation kept the GFP signal stable for up to 24 h. After washing with phosphate-buffered saline, floral meristems and gynoecia were individually harvested and mounted in water. The cover slip was gently pressed over each sample to slightly separate the cells from each other and facilitate visualization of the PIN localization.

For GUS staining, whole inflorescences were collected in ice-cold 90% (v/v) acetone and then prefixed by vacuum infiltration for 10 min. Tissues were then vacuum infiltrated with GUS staining solution without X-Gluc (50 mM $NaPO_4$, pH 7.2, 2 mM $Fe^{2+}CN$, 2 mM $Fe^{3+}CN$, and 0.2% [v/v] Triton X-100) for 10 min, then vacuum infiltrated in GUS staining solution supplemented with 2 mM X-Gluc for 10 min before incubation overnight at 37°C. Tissues were subsequently cleared in an ethanol series of 20%, 35%, and 50% (v/v) ethanol for 30 min each, fixed with formaldehyde-acetic acid (50% [v/v] ethanol, 3.7% [v/v] formaldehyde, and 5% [v/v] acetic acid) for 30 min, and then further cleared in 70%, 80%, and 90% (v/v) ethanol for 30 min each before a final clearing in chloral hydrate (2.5 g of chloral hydrate in 30% [v/v] glycerol) for up to 2 weeks.

For valve and epidermal phenotype quantification, flowers were fixed in formaldehyde-acetic acid for 16 h at 4°C and then cleared in 90%, then 70% (v/v) ethanol for 15 min each. Flowers were then cleared in chloral hydrate solution (see above) for a minimum of 5 d before analysis. The gynoecia were dissected out and mounted in chloral hydrate before imaging.

Microscopy and Imaging

Confocal laser-scanning micrographs of floral meristems and young gynoecia (stages 5–8) were obtained with a Zeiss 780 Inverted Axio Observer with a supersensitive GaASp detector. For GFP and YFP detection, a 488-nm argon laser was used for excitation, and emissions were detected between 508 and 569 nm. For chlorophyll *a* autofluorescence, a 633-nm argon laser was used for excitation, and emissions were detected between 648 and 721 nm. Using a C-Apochromat 63× water immersion objective (numerical aperture, 1.2), confocal scans were performed with the pinhole at 1 Airy unit. Presented images show either a single focal plane or a three-dimensional reconstruction of individual images taken as a z-series and processed using the ZEN2011 software.

The expression of fluorescent reporters in older gynoecia (stages 9–12) was analyzed using a Leica DMI4000 inverted microscope (HXC PL fluotar 10× objective) with differential interference contrast (DIC; Nomarski) optics, a Leica DFC360FX camera, and LAS AF (Leica Microsystems) software. For GFP and YFP detection, an L5 fluorescein isothiocyanate/GFP band-pass filter was used, and a rhodamine/red fluorescent protein long-pass filter was used for detecting chlorophyll autofluorescence.

GUS staining was analyzed using a Zeiss Axioplan microscope with DIC (Nomarski) optics, a Leica DFC295 camera, and LAS core imaging software. Epidermal cell phenotypes were analyzed using a Zeiss Axioscope A1 with DIC optics.

Adobe Illustrator CS6 and Photoshop CS6 were used to merge images to allow visualization of late-stage gynoecia, remove background from overview images, add arrows to indicate details, and assemble photographs.

Supplemental Data

The following materials are available in the online version of this article.

Supplemental Figure S1. The expression of *DR5rev:GFP* is identical to that of *DR5rev:3xVENUS-N7* during early gynoecial development.

Supplemental Figure S2. $PIN3_{pro}$:*PIN3-GFP* and $PIN7_{pro}$:*PIN7-GFP* are expressed in the basal part of gynoecia at floral stage 6.

Supplemental Figure S3. *DR5* expression after NPA treatment.

Supplemental Figure S4. The mediolateral axis is shifted 2 weeks after NPA treatment.

Supplemental Figure S5. Loss of *PGP1* and *PGP19* leads to disorganized epidermal cell patterning in both medial and lateral gynoecial tissues.

Supplemental Figure S6. Loss of *PGP1* and *PGP19* results in a reduced frequency of valveless gynoecia developed after NPA treatment.

ACKNOWLEDGMENTS

We thank Lars Østergaard (John Innes Centre) for technical advice concerning confocal imaging and for thoughtful comments on this article; Malcom Bennett (University of Nothingham), Annelie Carlsbecker (Uppsala University), Anna Stepanova (North Carolina State University), Antonio Martinez-Laborda (Universidad Miguel Hernández), Hélène Robert-Boisivon (Central-European Technology Institute), and Jiří Friml (Institute of Science and Technology) for kindly providing seeds; Anna Stepanova (North Carolina State University), Javier Brumos (North Carolina State University), Linda Robles (North Carolina State University), and Jose Alonso (North Carolina State University) for the parent vector and responder line used to create the *SHP2pro:GAL4/pUAS:3xYFP* two-component *SHP2* reporter; and the two anonymous reviewers for helpful and constructive comments on the article.

Received July 3, 2014; accepted October 18, 2014; published October 20, 2014.

LITERATURE CITED

Alonso-Cantabrana H, Ripoll JJ, Ochando I, Vera A, Ferrándiz C, Martínez-Laborda A (2007) Common regulatory networks in leaf and fruit patterning revealed by mutations in the Arabidopsis ASYMMETRIC LEAVES1 gene. Development **134:** 2663–2671

Bailly A, Sovero V, Geisler M (2006) The twisted dwarf's ABC: how immunophilins regulate auxin transport. Plant Signal Behav **1:** 277–280

Balanzá V, Navarrete M, Trigueros M, Ferrándiz C (2006) Patterning the female side of Arabidopsis: the importance of hormones. J Exp Bot **57:** 3457–3469

Benková E, Michniewicz M, Sauer M, Teichmann T, Seifertová D, Jürgens G, Friml J (2003) Local, efflux-dependent auxin gradients as a common module for plant organ formation. Cell **115:** 591–602

Bennett SRM, Alvarez J, Bossinger G, Smyth DR (1995) Morphogenesis in pinoid mutants of *Arabidopsis thaliana*. Plant J **8:** 505–520

Bishopp A, Help H, El-Showk S, Weijers D, Scheres B, Friml J, Benková E, Mähönen AP, Helariutta Y (2011) A mutually inhibitory interaction between auxin and cytokinin specifies vascular pattern in roots. Curr Biol **21:** 917–926

Blakeslee JJ, Bandyopadhyay A, Lee OR, Mravec J, Titapiwatanakun B, Sauer M, Makam SN, Cheng Y, Bouchard R, Adamec J, et al (2007) Interactions among PIN-FORMED and P-glycoprotein auxin transporters in *Arabidopsis*. Plant Cell **19:** 131–147

Blilou I, Xu J, Wildwater M, Willemsen V, Paponov I, Friml J, Heidstra R, Aida M, Palme K, Scheres B (2005) The PIN auxin efflux facilitator network controls growth and patterning in Arabidopsis roots. Nature **433:** 39–44

Bowman JL, Baum SF, Eshed Y, Putterill J, Alvarez J (1999) Molecular genetics of gynoecium development in Arabidopsis. Curr Top Dev Biol **45:** 155–205

Cheng Y, Dai X, Zhao Y (2006) Auxin biosynthesis by the YUCCA flavin monooxygenases controls the formation of floral organs and vascular tissues in Arabidopsis. Genes Dev **20:** 1790–1799

Dinneny JR, Weigel D, Yanofsky MF (2005) A genetic framework for fruit patterning in *Arabidopsis thaliana*. Development **132:** 4687–4696

Ferrándiz C, Pelaz S, Yanofsky MF (1999) Control of carpel and fruit development in Arabidopsis. Annu Rev Biochem **68:** 321–354

Friml J, Vieten A, Sauer M, Weijers D, Schwarz H, Hamann T, Offringa R, Jürgens G (2003) Efflux-dependent auxin gradients establish the apical-basal axis of Arabidopsis. Nature **426:** 147–153

Furutani M, Nakano Y, Tasaka M (2014) MAB4-induced auxin sink generates local auxin gradients in Arabidopsis organ formation. Proc Natl Acad Sci USA **111:** 1198–1203

Geisler M, Bailly A (2007) Tête-à-tête: the function of FKBPs in plant development. Trends Plant Sci **12:** 465–473

Geisler M, Blakeslee JJ, Bouchard R, Lee OR, Vincenzetti V, Bandyopadhyay A, Titapiwatanakun B, Peer WA, Bailly A, Richards EL, et al (2005) Cellular efflux of auxin catalyzed by the Arabidopsis MDR/PGP transporter AtPGP1. Plant J **44:** 179–194

Geisler M, Kolukisaoglu HÜ, Bouchard R, Billion K, Berger J, Saal B, Frangne N, Koncz-Kalman Z, Koncz C, Dudler R, et al (2003) TWISTED DWARF1, a unique plasma membrane-anchored immunophilin-like protein, interacts with Arabidopsis multidrug resistance-like transporters AtPGP1 and AtPGP19. Mol Biol Cell **14:** 4238–4249

Girin T, Sorefan K, Østergaard L (2009) Meristematic sculpting in fruit development. J Exp Bot **60:** 1493–1502

González-Reig S, Ripoll JJ, Vera A, Yanofsky MF, Martínez-Laborda A (2012) Antagonistic gene activities determine the formation of pattern elements along the mediolateral axis of the Arabidopsis fruit. PLoS Genet **8:** e1003020

Habets MEJ, Offringa R (2014) PIN-driven polar auxin transport in plant developmental plasticity: a key target for environmental and endogenous signals. New Phytol **203:** 362–377

Hawkins C, Liu Z (2014) A model for an early role of auxin in Arabidopsis gynoecium morphogenesis. Front Plant Sci **5:** 327

Hay A, Barkoulas M, Tsiantis M (2006) ASYMMETRIC LEAVES1 and auxin activities converge to repress BREVIPEDICELLUS expression and promote leaf development in Arabidopsis. Development **133:** 3955–3961

Heisler MG, Ohno C, Das P, Sieber P, Reddy GV, Long JA, Meyerowitz EM (2005) Patterns of auxin transport and gene expression during primordium development revealed by live imaging of the Arabidopsis inflorescence meristem. Curr Biol **15:** 1899–1911

Kim JY, Henrichs S, Bailly A, Vincenzetti V, Sovero V, Mancuso S, Pollmann S, Kim D, Geisler M, Nam HG (2010) Identification of an ABCB/P-glycoprotein-specific inhibitor of auxin transport by chemical genomics. J Biol Chem **285:** 23309–23317

Larsson E, Franks RG, Sundberg E (2013) Auxin and the *Arabidopsis thaliana* gynoecium. J Exp Bot **64:** 2619–2627

Marsch-Martínez N, Ramos-Cruz D, Irepan Reyes-Olalde J, Lozano-Sotomayor P, Zúñiga-Mayo VM, de Folter S (2012) The role of cytokinin during Arabidopsis gynoecia and fruit morphogenesis and patterning. Plant J **72:** 222–234

Mattsson J, Ckurshumova W, Berleth T (2003) Auxin signaling in Arabidopsis leaf vascular development. Plant Physiol **131:** 1327–1339

Moschou PN, Smertenko AP, Minina EA, Fukada K, Savenkov EI, Robert S, Hussey PJ, Bozhkov PV (2013) The caspase-related protease separase (extra spindle poles) regulates cell polarity and cytokinesis in *Arabidopsis*. Plant Cell **25:** 2171–2186

Mravec J, Kubeš M, Bielach A, Gaykova V, Petrásek J, Skůpa P, Chand S, Benková E, Zazímalová E, Friml J (2008) Interaction of PIN and PGP transport mechanisms in auxin distribution-dependent development. Development **135:** 3345–3354

Murphy AS, Hoogner KR, Peer WA, Taiz L (2002) Identification, purification, and molecular cloning of *N*-1-naphthylphthalmic acid-binding plasma membrane-associated aminopeptidases from Arabidopsis. Plant Physiol **128:** 935–950

Nagashima A, Uehara Y, Sakai T (2008) The ABC subfamily B auxin transporter AtABCB19 is involved in the inhibitory effects of *N*-1-naphthyphthalamic acid on the phototropic and gravitropic responses of Arabidopsis hypocotyls. Plant Cell Physiol **49:** 1250–1255

Nemhauser JL, Feldman LJ, Zambryski PC (2000) Auxin and ETTIN in Arabidopsis gynoecium morphogenesis. Development **127:** 3877–3888

Noh B, Murphy AS, Spalding EP (2001) Multidrug resistance-like genes of *Arabidopsis* required for auxin transport and auxin-mediated development. Plant Cell **13:** 2441–2454

Nole-Wilson S, Azhakanandam S, Franks RG (2010) Polar auxin transport together with aintegumenta and revoluta coordinate early Arabidopsis gynoecium development. Dev Biol **346:** 181–195

Okada K, Ueda J, Komaki MK, Bell CJ, Shimura Y (1991) Requirement of the auxin polar transport system in early stages of *Arabidopsis* floral bud formation. Plant Cell **3:** 677–684

Ori N, Eshed Y, Chuck G, Bowman JL, Hake S (2000) Mechanisms that control knox gene expression in the Arabidopsis shoot. Development **127:** 5523–5532

Østergaard L (2009) Don't 'leaf' now. The making of a fruit. Curr Opin Plant Biol **12:** 36–41

Petrásek J, Cerná A, Schwarzerová K, Elčkner M, Morris DA, Zazímalová E (2003) Do phytotropins inhibit auxin efflux by impairing vesicle traffic? Plant Physiol **131:** 254–263

Reinhardt D, Pesce ER, Stieger P, Mandel T, Baltensperger K, Bennett M, Traas J, Friml J, Kuhlemeier C (2003) Regulation of phyllotaxis by polar auxin transport. Nature **426:** 255–260

Roeder AH, Ferrándiz C, Yanofsky MF (2003) The role of the REPLUMLESS homeodomain protein in patterning the Arabidopsis fruit. Curr Biol **13:** 1630–1635

Sachs T (1969) Polarity and the induction of organized vascular tissues. Ann Bot (Lond) **33:** 263–275

Scarpella E, Marcos D, Friml J, Berleth T (2006) Control of leaf vascular patterning by polar auxin transport. Genes Dev **20:** 1015–1027

Schneitz K, Hülskamp M, Pruitt RE (1995) Wild-type ovule development in *Arabidopsis thaliana*: a light microscope study of cleared whole-mount tissue. Plant J **7:** 731–749

Sessions R (1997) Arabidopsis (Brassicaceae) flower development and gynoecium patterning in wild type and Ettin mutants. Am J Bot **84:** 1179

Sessions RA, Zambryski PC (1995) Arabidopsis gynoecium structure in the wild and in ettin mutants. Development **121:** 1519–1532

Smyth DR, Bowman JL, Meyerowitz EM (1990) Early flower development in *Arabidopsis*. Plant Cell **2:** 755–767

Sohlberg JJ, Myrenås M, Kuusk S, Lagercrantz U, Kowalczyk M, Sandberg G, Sundberg E (2006) STY1 regulates auxin homeostasis and affects apical-basal patterning of the Arabidopsis gynoecium. Plant J **47:** 112–123

Ståldal V, Sohlberg JJ, Eklund DM, Ljung K, Sundberg E (2008) Auxin can act independently of CRC, LUG, SEU, SPT and STY1 in style development but not apical-basal patterning of the Arabidopsis gynoecium. New Phytol **180:** 798–808

Stepanova AN, Robertson-Hoyt J, Yun J, Benavente LM, Xie DY, Dolezal K, Schlereth A, Jürgens G, Alonso JM (2008) TAA1-mediated auxin biosynthesis is essential for hormone crosstalk and plant development. Cell **133:** 177–191

Su YH, Liu YB, Zhang XS (2011) Auxin-cytokinin interaction regulates meristem development. Mol Plant **4:** 616–625

Sundberg E, Ferrandíz C (2009) Gynoecium patterning in Arabidopsis: a basic plan behind a complex structure. *In* L Østergaard, ed, Fruit Development and Seed Dispersal, Vol 38. Annual Plant Reviews Oxford, pp 35–69

Sundberg E, Østergaard L (2009) Distinct and dynamic auxin activities during reproductive development. Cold Spring Harb Perspect Biol **1:** a001628

Ulmasov T, Murfett J, Hagen G, Guilfoyle TJ (1997) Aux/IAA proteins repress expression of reporter genes containing natural and highly active synthetic auxin response elements. Plant Cell **9:** 1963–1971

Vernoux T, Brunoud G, Farcot E, Morin V, Van den Daele H, Legrand J, Oliva M, Das P, Larrieu A, Wells D, et al (2011) The auxin signalling network translates dynamic input into robust patterning at the shoot apex. Mol Syst Biol **7:** 508

Vieten A, Vanneste S, Wisniewska J, Benková E, Benjamins R, Beeckman T, Luschnig C, Friml J (2005) Functional redundancy of PIN proteins is accompanied by auxin-dependent cross-regulation of PIN expression. Development **132:** 4521–4531

Wang B, Bailly A, Zwiewka M, Henrichs S, Azzarello E, Mancuso S, Maeshima M, Friml J, Schulz A, Geisler M (2013) *Arabidopsis* TWISTED DWARF1 functionally interacts with auxin exporter ABCB1 on the root plasma membrane. Plant Cell **25:** 202–214

Watanabe K, Okada K (2003) Two discrete *cis* elements control the Abaxial side-specific expression of the *FILAMENTOUS FLOWER* gene in *Arabidopsis*. Plant Cell **15:** 2592–2602

Yanai O, Shani E, Dolezal K, Tarkowski P, Sablowski R, Sandberg G, Samach A, Ori N (2005) Arabidopsis KNOXI proteins activate cytokinin biosynthesis. Curr Biol **15:** 1566–1571

Zádníková P, Petrásek J, Marhavý P, Raz V, Vandenbussche F, Ding Z, Schwarzerová K, Morita MT, Tasaka M, Hejátko J, et al (2010) Role of PIN-mediated auxin efflux in apical hook development of *Arabidopsis thaliana*. Development **137:** 607–617

Zúñiga-Mayo VM, Reyes-Olalde JI, Marsch-Martinez N, de Folter S (2014) Cytokinin treatments affect the apical-basal patterning of the Arabidopsis gynoecium and resemble the effects of polar auxin transport inhibition. Front Plant Sci **5:** 191